Available online at www.sciencedirect.com

SCIENCE DIRECT

Developmental Biology 283 (2005) 85 – 96

DEVELOPMENTAL BIOLOGY

www.elsevier.com/locate/ydbio

15-Zinc finger protein Bloody Fingers is required for zebrafish morphogenetic movements during neurulation

Saulius Sumanas[a], Bo Zhang[a,b], Rujuan Dai[a], Shuo Lin[a,*]

[a]*University of California, Los Angeles, Department of Molecular, Cell and Developmental Biology, 621 C. Young Dr. South, Los Angeles, CA 90095, USA*
[b]*College of Life Sciences, Peking University, Beijing 100871, China*

Received for publication 15 December 2004, revised 17 March 2005, accepted 5 April 2005
Available online 10 May 2005

Abstract

A novel zebrafish gene *bloody fingers (blf)* encoding a 478 amino acid protein containing fifteen C_2H_2 type zinc fingers was identified by expression screening. As determined by in situ hybridization, *blf* RNA displays strong ubiquitous early zygotic expression, while during late gastrulation and early somitogenesis, *blf* expression becomes transiently restricted to the posterior dorsal and lateral mesoderm. During later somitogenesis, *blf* expression appears only in hematopoietic cells. It is completely eliminated in *cloche, moonshine* but not in *vlad tepes (gata1)* mutant embryos. Morpholino (MO) knockdown of the Blf protein results in the defects of morphogenetic movements. Blf-MO-injected embryos (morphants) display shortened and widened axial tissues due to defective convergent extension. Unlike other convergent extension mutants, *blf* morphants display a split neural tube, resulting in a phenotype similar to the human open neural tube defect spina bifida. In addition, dorsal ectodermal cells delaminate in *blf* morphants during late somitogenesis. We propose a model explaining the role of *blf* in convergent extension and neurulation. We conclude that *blf* plays an important role in regulating morphogenetic movements during gastrulation and neurulation while its role in hematopoiesis may be redundant.

Keywords: Zebrafish; Convergent extension; Neurulation; Zinc finger; Gastrulation; Neural tube; Spina bifida; Blood; Hematopoietic

Introduction

Morphogenetic movements accompanied by coordinated cell migration and cell shape changes lead to the establishment of the body axis during vertebrate development. During zebrafish gastrulation, prospective mesendodermal cells involute and ingress. This is followed by convergence and extension movements in which mesendoderm and ectoderm undergo cell intercalations along the medial–lateral axis that narrow the tissues and consequently extend them along the anterior–posterior axis (reviewed in Heisenberg and Tada, 2002). Gastrulation is followed by neurulation during which the neural plate is specified and transformed into neural tube. In contrast to other vertebrates, neural folds are not evident in zebrafish; instead, a neural keel is formed (reviewed in Strahle and Blader, 1994). The neural tube is then shaped by oriented cell divisions and convergent extension (CE) movements. It has been proposed that the mechanism of teleost neurulation is similar to the secondary neurulation seen in the tailbud of higher vertebrates. However, recent studies have demonstrated the epithelial origin of the zebrafish neural keel, arguing that zebrafish neural tube formation may be just a variant of primary neurulation (Papan and Campos-Ortega, 1994; Reichenbach et al., 1990; reviewed in Lowery and Sive, 2004).

Several zebrafish mutants have been identified which exhibit defects in convergent extension. Among them are *pipetail (ppt)*, *knypek (kny)*, and *trilobite (tri)* mutant embryos which exhibit a shortened body axis from late gastrulation stages onwards (Hammerschmidt et al., 1996; Marlow et al., 1998; Solnica-Krezel et al., 1996). These loci have been shown to encode *wnt5*, *glypican knypek*, and *strabismus*, respectively, components or modulators of the

* Corresponding author. Fax: +1 310 267 4971.
E-mail address: shuolin@ucla.edu (S. Lin).

0012-1606/$ - see front matter © 2005 Elsevier Inc. All rights reserved.
doi:10.1016/j.ydbio.2005.04.007

wnt non-canonical signaling pathway (Jessen et al., 2002; Rauch et al., 1997; Topczewski et al., 2001). This pathway is analogous to the planar cell polarity (PCP) pathway in *Drosophila* and is thought to regulate convergent extension movements in vertebrates (Darken et al., 2002; Heisenberg et al., 2000; Park and Moon, 2002; Shulman et al., 1998; Wallingford et al., 2000). Some other transducers or modulators of the PCP pathway have also been shown to affect convergent extension in zebrafish including Frizzled-2 (Fz2) and Prickle (Pk) proteins (Carreira-Barbosa et al., 2003; Kilian et al., 2003; Sumanas et al., 2001; Veeman et al., 2003).

Defects in convergent extension and neurulation are known to cause embryo abnormalities in many vertebrates, including humans. Incomplete closure of the neural tube, spina bifida, is among the most common birth defects contributing to infant mortality and serious disability (Copp et al., 2003). Mutations in the mouse orthologs of the *Drosophila* PCP genes *disheveled*, *strabismus*, *scribble*, and *flamingo*, all result in failure to initiate neural tube closure (Ueno and Greene, 2003). Loss of function of *wnt*, *frizzled-7*, *disheveled*, *strabismus*, and *prickle* has been shown to perturb gastrulation movements and result in open neural tube in *Xenopus* (Hoppler et al., 1996; Goto and Keller, 2002; Sumanas et al., 2000; Takeuchi et al., 2003; Wallingford and Harland, 2002; Winklbauer et al., 2001). These data demonstrate the involvement of the PCP pathway in regulating both convergent extension and neurulation and illustrates the interdependence of both fundamental processes of morphogenesis in different vertebrates. However, the open neural tube phenotype has not been described in the zebrafish as yet.

In the current study, we have identified a gene encoding a novel zebrafish multiple C_2H_2 zinc finger protein family member, *Bloody fingers (Blf)*. Zinc finger proteins contain a small peptide domain with a special secondary structure stabilized by a zinc ion bound to Cys and His residues of the finger (reviewed in Iuchi, 2001). The most common type of zinc fingers, C_2H_2, is primarily involved in DNA binding and transcriptional regulation. There are hundreds of different C_2H_2 proteins in vertebrate genomes. One of the subclasses of C_2H_2 proteins includes multiple-adjacent C_2H_2 zinc finger proteins. Members of this subclass can have as many as 29 adjacent zinc fingers such as in the protein Roaz (Tsai and Reed, 1997). In addition to DNA binding, zinc fingers in these proteins can also engage in protein–protein interactions to promote homo- or hetero-dimerization such as the one observed between the blood-specific Ikaros protein and two of its homologues, Alios and Helios (Kelley et al., 1998; Morgan et al., 1997). Some of the multiple C_2H_2 domain proteins are also known to bind single-stranded or double-stranded RNA, e.g., TFIIIA and dsRBP-Zfa proteins (Finerty and Bass, 1997; Friesen and Darby, 1998).

Blf protein is predicted to contain 15 sequential zinc fingers spanning almost the entire length of the protein with no other motives detectable. *Blf* RNA is expressed ubiquitously in early zebrafish embryos and is progressively restricted to the posterior dorsal and lateral mesoderm during gastrulation while later expressed in the hematopoietic progenitor cells. Knockdown of Blf protein using antisense morpholino oligonucleotides (MOs) revealed its critical role in convergent extension and neurulation movements. Blf-MO-injected embryos display shortened body axis, split neural tube similar to the spina bifida condition in humans, and delaminating dorsal ectodermal cells. This is the first time that a phenotype similar to spina bifida has been demonstrated in zebrafish suggesting that zebrafish can be used to model this human birth defect. We also propose a model explaining how defective convergent extension results in the open neural tube of *blf* morphants.

Materials and methods

Blf clone isolation

A cDNA clone of 1.92 kb encompassing a short stretch of the 5′UTR, the complete putative ORF sequence of *blf* and the 3′UTR was isolated from the zebrafish embryonic blood cell-specific cDNA library (Long et al., 2000). Using the 5′RACE kit (Promega), an additional 5′UTR sequence was isolated from synthesized cDNA derived from total purified RNA of 24 hpf zebrafish embryos. The combined size of the isolated *blf* cDNA and a predicted poly-A tail of 200–300 nucleotides is in close agreement with the experimentally observed *blf* size of ~2.4 kb, as determined by Northern blotting, suggesting that the complete *blf* cDNA sequence was isolated.

In situ hybridization

In situ hybridization was performed as described (Jowett, 1999). To synthesize DIG-labeled antisense *blf* probe, a *blf*-pTriplEx (Clontech) construct was linearized with *Kpn*I and transcribed with T7 RNA polymerase (Promega). Other probes used include: *no tail (ntl)* (Schulte-Merker et al., 1994); *sonic hedgehog (shh)* (Ekker et al., 1995); *spondin-1b (spon1b)* (Higashijima et al., 1997); *myod* (Weinberg et al., 1996); *crestin* (Luo et al., 2001); cb497 cDNA, corresponding to *hairy-related 4 (her4)* (Thisse et al., 2001); cb112 cDNA, similar to *cytokeratin E7* (Thisse et al., 2001); *gata1* (Detrich et al., 1995); *gata2* (Detrich et al., 1995); *tal1 (scl)* (Liao et al., 1998); *cmyb* (Thompson et al., 1998); and *ikaros* (Willett et al., 2001). To synthesize a probe for the *forkhead box A1 (foxa1)*, the ORF of *foxa1* was amplified by PCR from the post-somitogenesis stage cDNA library (kindly donated by S. C. Ekker), subcloned into the 4-TOPO vector (Invitrogen), linearized with *Spe*I, and transcribed using T7 RNA polymerase.

```
blf         MSDPETSIMD QEDLSDLMEE SEESEEMSEV EKKRRHVKTP KTSQTKSAQK   50
draculin    MKNTTKPCRT EHH------- --------NA EGQRDRMEGN KKGETK-AKK   34

blf         TFKCPQCGKK FARKSGLTAH VKIHTGEKPF SCKECGKSFS SSGYIKRHMI  100
draculin    SVACSHCKKR FTHKVHLQIH MRVHTGEKPY RCDQCGKCFP YKQSLKLHLD   84

blf         IHSGEKPHTC DQCGKSFGLA SSLKSHAAVH SEEKPFKCDH CGDSFRWLSS  150
draculin    IHAKGNPYTC DECGESFKTR LQLRSHMTLH PKYKPYKCDQ CEKSYGREDH  134

blf         LRDHLKTHGK KETHVCSVCG KSFAQLILLK KHKKRHEVKN FMCFECGKTF  200
draculin    LQRHMKLHTG EKPHKCEHCG KSFPMRDLLR SHLMVH---- ----------  168

blf         VRNCELKQHQ RVHTGEKPYK CSHCDKRFSN GSSKVVHERI HTGERPYSCD  250
draculin    ---------- ---SEVKPYT CDQCGKGFTL KKSYNEHMNI HTGERPYTCD  207

blf         QCGHAFRHTH ALESHKRIHT GEKSYTCDQC GKSFTQKASL RIHKKFHNAE  300
draculin    QCGKGFPYEQ SLNLHMRFHR EEKPFTCDQC GQSFSQKGAY NIHMKIHTGE  257

blf         KPHTCDQCGK SFTLKTSLNE HMKIHTGEKP HTCDQCGKRF SRLSLLKLHL  350
draculin    KPYTCDQCGM SFRHGYSLKL HMTHHTGEKP FHCDQCDKCY STALFLKNHI  307

blf         ATHSVIRPYR CEKCGKGFTW ESCLKNHLKT HSEEKPHKCS VCGKGFRLAN  400
draculin    KTHDKAQIYS CLTCGKTFNQ LRGLRLHEKR HSLTKPFMCF DCGKCYFTDT  357

blf         SLRSHQKRHT GVKNHMCFDC GKTYFTKNEL KLHQKVHSGG EFYKCLHCDM  450
draculin    ELKQHLPVHS NERPYMCSLC FKSFPRMGSL IVHEKTHNGE ---KP-DC--  401

blf         TFKRLDYVKN HEKTHTVRSD PSESSEED                          478
draculin    ---------- -------RTG -SKKSQDE                          411
```

Fig. 1. Alignment of the putative amino acid sequences of the zebrafish Bloody Fingers and Draculin proteins. Blf contains 15 sequential zinc finger domains while Draculin contains 13. Zinc finger domains are marked against gray background, zinc binding Cys and His residues are marked in red. Sequences were aligned using GeneWorks 2.5 software. *Blf* sequence has been submitted to GenBank under the accession number AY523041.

Northern blotting

Northern hybridization was performed as described (Hopwood et al., 1989). Total RNA purified from 10 embryos was loaded on a denaturing agarose gel for each stage analyzed. To synthesize *blf* probe, the ORF of *blf* was amplified by PCR, subcloned into the *Spe*I site of pT3TS (Hyatt and Ekker, 1999). The *blf*-T3TS/*Spe*I fragment was then labeled with ^{32}P and used as a probe. Ethidium bromide staining of ribosomal RNA was used as a loading control.

MO injection

Three *blf*-specific MOs, MO1 (TGGATCACT-CATTTTCTCTGTGTTC), MO2 (TTTCTCTGTGTTC-TCCCTCCACTTG), MO3 (TTATGCTGGTTTCTG-GATCACTCAT), and the 5-base MO2 mismatch (TTTCACTGTCTTCTGCCTGCACTAG) were used to study the function of Blf protein. 2–4 ng of 1 mg/ml MO solution in Danieau buffer (Nasevicius and Ekker, 2000) supplemented with 15 mM Tris–Cl (pH 7.5) was microinjected into zebrafish embryos at the one-cell to two-cell stage as described (Hyatt and Ekker, 1999).

To inhibit the function of *draculin*, 5–10 ng of *dra1* and *dra2* MOs (CAGGGTTTTGTTGTATTCTTCATCT and TCACGCTTTTCTCTATTTCCAAGTG) was injected. Also, the following combinations of *blf* and *dra* MOs were injected: 2–4 nl *blf* MO2/*dra1* MO, 1:2 ratio, 1 mg/ml total MO concentration; 2–4 nl *blf* MO2/*dra2* MO, 1:4 ratio, 1 mg/ml total; and 1–4 nl *blf* MO2/*blf* MO3/*dra1* MO/*dra2* MO, 1:1:1:1 ratio, 1 mg/ml total. The ratios were chosen to minimize non-specific MO effects observed at higher doses.

Cell-tracing

Cell labeling with DMNB-caged fluorescein dextran (Mw 10,000, Molecular Probes) was performed as described (Yamashita et al., 2002).

Real-time RT-PCR

To analyze gene expression level, batches of ten 2.5 ng *blf* MO2, 7.5 ng *blf* MO3-injected and uninjected control embryos were frozen on dry ice at the 10-somite stage. Total RNA was purified using the RNAquous-4PCR kit (Ambion). cDNA was synthesized using a mix of random hexamers (Roche) and the Powerscript reverse transcriptase (BD Biosciences). Real-time PCR was performed using the iCycler iQ Real-Time PCR Detection System (Bio-Rad) and the iQ SYBR Green Supermix (Biorad). Relative cDNA amounts were calculated using the iCycler program

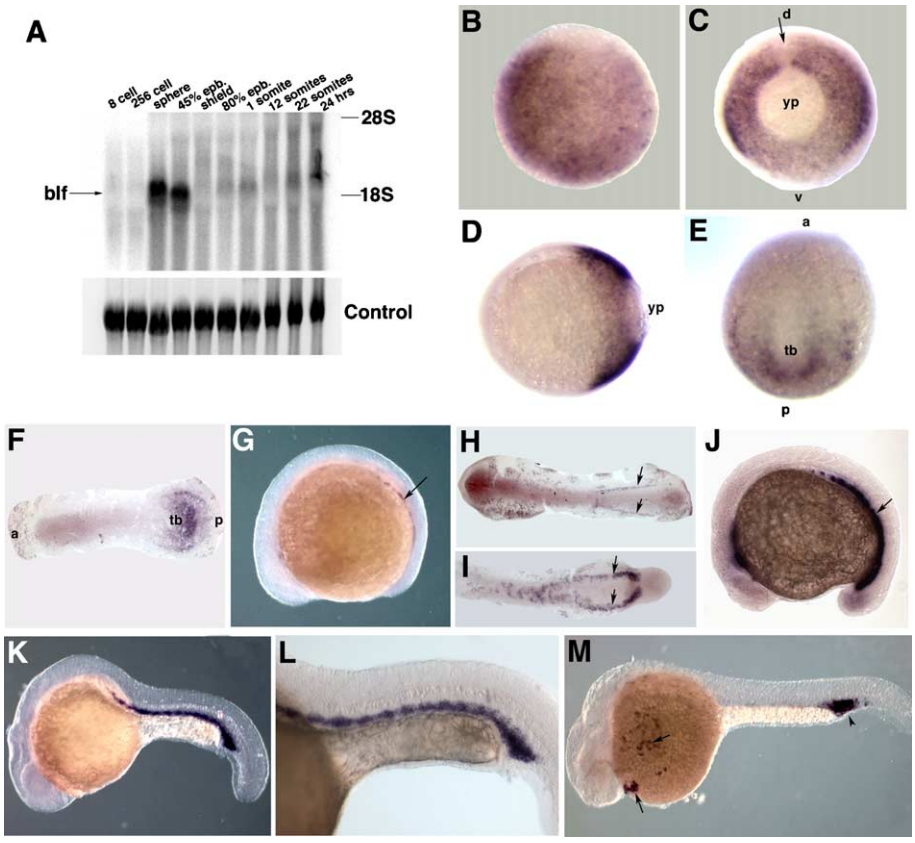

Fig. 2. Analysis of the *blf* expression pattern. (A) Northern blotting analysis of *blf* expression. A single *blf*-specific band of ~2.4 kb size is observed from the sphere stage onwards. Maximum expression is observed at the sphere and 45% epiboly stages. 28S and 18S rRNA bands are indicated. (B–M) In situ hybridization analysis of *blf* expression. Anterior is to the left except where indicated. (B) 50% epiboly stage, animal view. *blf* expression appears uniform and ubiquitous within the blastoderm. (C, D) 80% epiboly stage, (C) vegetal view, (D) lateral view. *blf* is expressed within the posterior hypoblast and excluded from the dorsalmost cells (arrow, C). d, dorsal; v, ventral; yp, yolk plug. (E) 1-somite stage, dorso-posterior view. *blf* is localized to the posterior dorsal paraxial and lateral mesoderm and excluded from the axial mesoderm. Expression extends into the ventral region close to the tailbud (tb). a, anterior, p, posterior. (F) 3-somite stage, flat mount. *blf* is expressed in a semicircular pattern around the tailbud region (tb) in the dorsal paraxial and lateral mesoderm. a, anterior, p, posterior. (G, H) 10-somite stage. *blf* is expressed in two stripes of the putative hematopoietic progenitor cells in ventrolateral mesoderm (arrows). (I) 18-somite stage, the tail region. *blf* is localized to two stripes within the hematopoietic region of ventrolateral mesoderm. (J) 15-somite stage. *blf* is expressed in the presumptive hematopoietic cells in ventrolateral posterior mesoderm. (K, L) 22 hpf stage. *blf* is localized to the intermediate cell mass (ICM) region, where the primitive hematopoiesis is known to take place. (M) 26 hpf stage. *blf* is expressed in the ICM region (arrowhead) and circulating blood cells (arrows).

(Bio-Rad) and normalized to the expression of elongation factor 1α (EF1α). The following primer pairs were used: *her4* AAGACACACAGCAATGACTCC, ACTAAAGCCGTGTGGTCATCG; *ngn1* AGACTCTGCGCTTCGCTCAC, TTCTGGAGATTCTATACCGAC; *foxb1.2* CGCCATCGAGAACATCATCG, CAGAGATTGCGGAGAGTTCG; *crestin* TTAGGATTGACTCCTTTCACC, TCTAAGCATGCGCGAGATGTG; *gata3* TCAACCTTGAAGCCTCGCAC, GAGTCATTCCACCTTGCAGG; *cytokeratin E7* ATCTGCGCAAGAAAATCTCC, ACTGCTGTCGCATCTCCTCC; and *EF1α* TCACCCTGGGAGTGAAACAGC, ACTTGCAGGCGATGTGAGCAG. The following PCR profile was used: 95°C 3 min; 95°C 10 s, 58°C 30 s, 72°C 30 s (data acquisition point), repeat 40 times. In the case of *her4*, data acquisition was performed at 84°C. Specific amplification of each product was confirmed by gel and melting curve analysis.

Results

Isolation of the bloody fingers gene and its expression pattern

A zebrafish cDNA library was prepared from the purified hematopoietic progenitor cells using *gata1*-GFP transgenic zebrafish (Long et al., 2000). One of the isolated cDNA clones encoded a novel 478 amino acid protein, Bloody Fingers (Blf), containing fifteen sequential C_2H_2 type zinc finger domains which comprised almost the entire length of the protein (Fig. 1). No other homology domains were found using BLAST searches of protein databases. All of the 15 zinc fingers are highly conserved; each of them is 21 amino acid (a.a.) long linked by the 7 a.a. long linker region. Although these zinc finger domains are highly similar to the ones in multiple zinc finger proteins from other vertebrates,

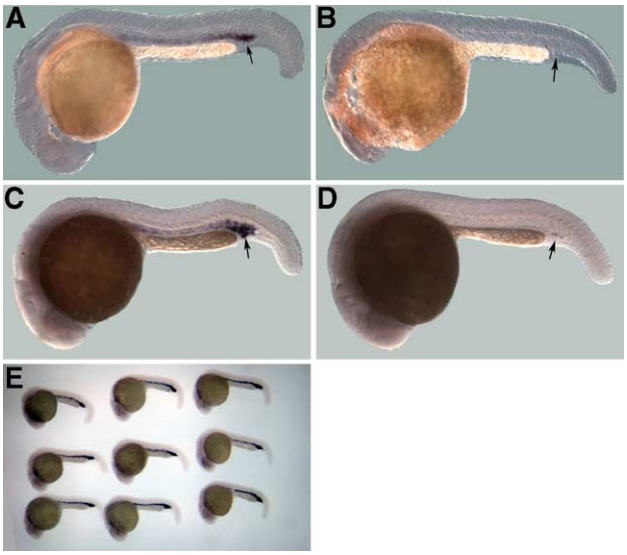

Fig. 3. Analysis of *blf* expression in hematopoietic mutants at 22 hpf. (A, B) *cloche* (*clo*^{m39}) homozygous embryos have lost *blf* expression. (A) ~3/4 of progeny from heterozygous *clo* carriers display *blf* expression in the ICM region (arrow) while (B) ~1/4 of embryos have very few or none *blf*-expressing cells. (C, D) *moonshine* (*mon*^{tu244b}) homozygous embryos defective in TIF1γ transcription factor have lost *blf* expression. (C) ~3/4 of progeny from heterozygous *mon* carriers display *blf* expression in the ICM region (arrow) while (D) ~1/4 of embryos have very few or none *blf*-expressing cells. (E) *blf* expression is not affected in the progeny from the *vlad tepes* (*vt*^{m651}) carriers defective in the *gata1* transcription factor.

we were unable to find a protein that has a similar structure of 15 zinc fingers from any other organism. The most structurally similar protein to Blf is the zebrafish protein Draculin, containing 13 sequential zinc finger domains (Herbomel et al., 1999) (Fig. 1). The two proteins share 42% similarity and 36% identity, displaying high homology in the zinc finger and most of the linker regions.

We investigated the expression pattern of *blf* using Northern blotting and in situ hybridization. No maternal expression was detected. A single band of ~2.4 kb was observed during most of the zygotic stages analyzed (Fig. 2A). The strongest expression of *blf* was noted immediately after the start of the zygotic transcription, at the sphere, 30% and 45% epiboly stages (Fig. 2A, and data not shown). Expression decreased dramatically afterwards. *blf* mRNA was distributed uniformly throughout the embryo from the sphere to the shield stages, as analyzed by in situ hybridization (Fig. 2B, and data not shown). During later epiboly stages, *blf* RNA gradually became excluded from the animal pole and the most dorsal region of the embryo (Figs. 2C, D). Between the tailbud and the 4 somite stages, *blf* mRNA became localized to the posterior dorsolateral and lateral mesoderm, surrounding the yolk plug in a semicircular pattern (Figs. 2E, F). Expression at those stages was restricted to the mesodermal cell layer as determined by section analysis (data not shown). The expression region became

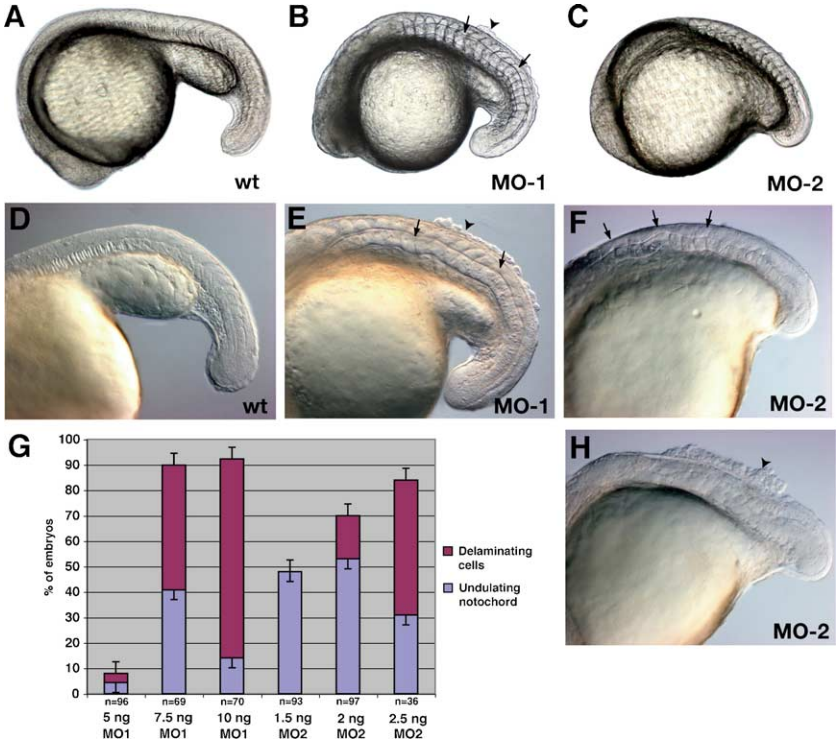

Fig. 4. Morphological analysis of *blf* morphants at the 22-somite stage. *Blf* MOs caused a minor general developmental delay; therefore, all embryos were staged individually by the standard staging criteria (Kimmel et al., 1995). (A, D) Control uninjected embryo, (B, E) 7.5 ng *blf* MO1-injected embryo, (C, F) 1.5 ng *blf* MO2-injected embryo, (H) 2ng *blf* MO2-injected embryo. Note the notochord and floorplate undulations (arrows), delaminating dorsal ectodermal cells (arrowheads) and the severely shortened axis in *blf* MO-injected embryos. (G) Percentage of *blf* MO-injected embryos displaying axial undulations and delaminating ectodermal cells. Embryos injected with a control 5-base mismatch *blf*-MO2 were completely normal (not shown). *blf*-MO3 also caused axial undulations, albeit at lower frequency (not shown).

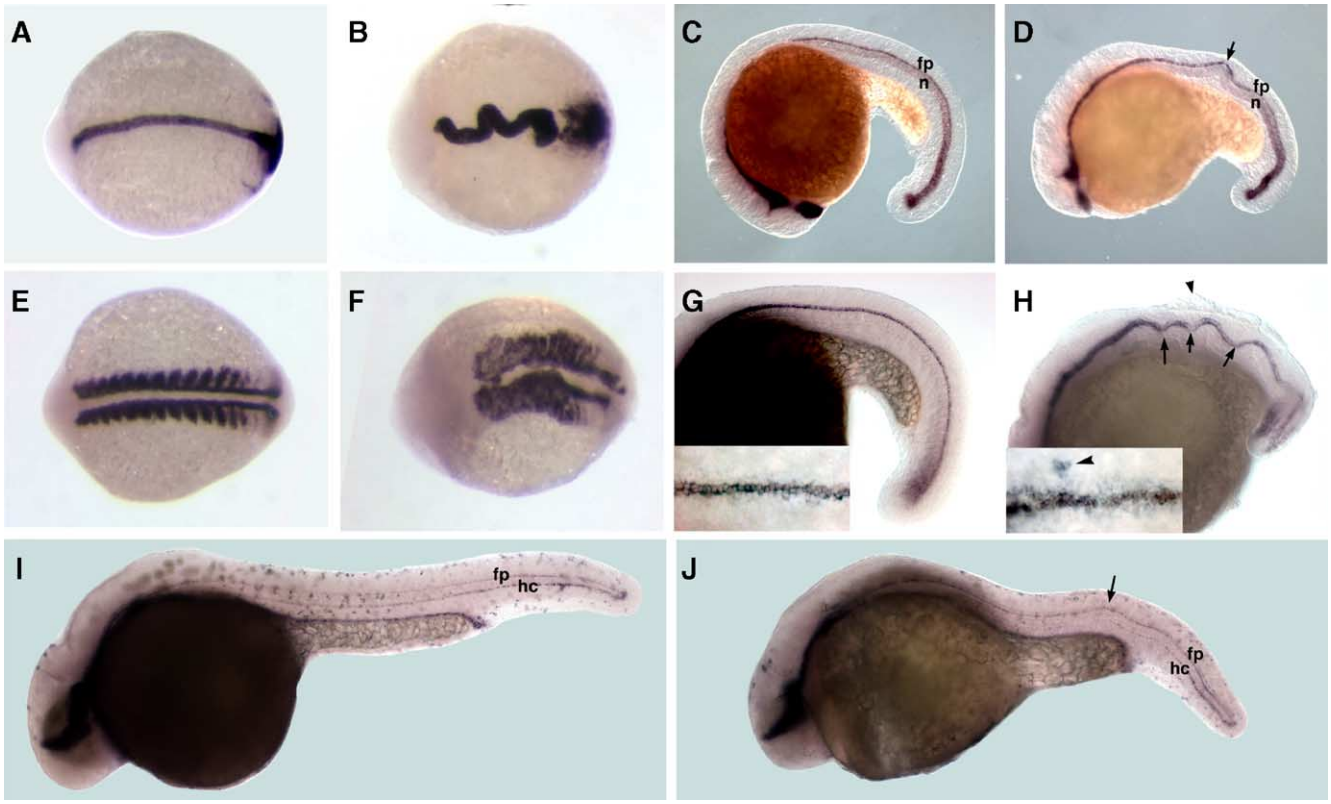

Fig. 5. In situ hybridization analysis of axial markers in *blf* morphants, injected with 2 ng of MO2. Anterior is to the left in all panels. (A, B) Notochord marked by *no tail (ntl)* expression at the 10-somite stage. Note the shortened, thickened, and undulating notochord in *blf* morphants (B), compared with control uninjected embryos (A). (C, D) *Sonic hedgehog (shh)* marks the notochord (n) and the floorplate (fp) at the 22-somite stage. Note the undulating notochord and floorplate in *blf* morphants (D), compared with control uninjected embryos (C). (E, F) *myod* expression marks paraxial somitic mesoderm at the 10-somite stage. Note wider and compressed somites as well as undulations in adaxial stripes of *myod*-expressing cells in *blf* morphants (F), compared with control uninjected embryos (E). (G, H) Expression of *spondin1b (spon1b)* marks the floorplate at the 22-somite stage. Note severe undulations (arrows) and delaminating cells (arrowhead) in *blf* morphants (H), compared to uninjected control embryos (G). Inset, high-magnification dorsal view of the floorplate. Note the wider and disorganized floorplate in the inset (H). A cluster of *spon1b*-expressing cells failed to converge to the midline (arrowhead, inset in H). (I, J) Expression of the *forkhead* family transcription factor *foxA1 (fkd7)* marks the floorplate (fp), the hypochord (hc), and endoderm at 24 hpf. Note undulations of the floorplate and the hypochord in *blf* morphants (J), compared with uninjected controls (I).

tighter around the yolk plug and gradually disappeared as embryos showed very little expression of *blf* during the 5–7 somite stages. *blf* expression reappeared at the 8-somite stage in two bilaterally symmetrical stripes within the posterior lateral mesoderm, the region where hematopoietic precursor cells are known to originate. This expression domain was spatially distinct from the earlier *blf* expression close to the tailbud region. Expression of *blf* in presumptive hematopoietic cell precursors grew stronger during later somitogenesis (Figs. 2G–L). As blood circulation began at 24 hpf, *blf* expression was observed in the intermediate cell mass as well as in the circulating blood cells (Fig. 2M). *blf* expression became much weaker shortly after that and was not detectable after 30 hpf (data not shown).

Blf expression in hematopoietic mutants

Based on the *blf* expression pattern in hematopoietic mesoderm, we analyzed *blf* expression in four different hematopoietic mutants. *Cloche (clo)* mutants form no blood cells or blood vessels, and are thought to affect one of the earliest steps in hemangioblast formation (Stainier et al., 1995; Thompson et al., 1998). *blf*-expressing cells were almost completely absent in ~1/4 of the progeny (16 out of 68 embryos) from clo^{m39} heterozygous carriers as analyzed by in situ hybridization at the 12–26 somite stages (Figs. 3A, B). *Moonshine/vampire (mon)* mutants are defective in the transcriptional intermediary factor 1γ (TIF1γ) and are bloodless at the onset of circulation (Ransom et al., 1996, 2004; Stainier et al., 1996). *blf* expression was almost completely absent in ~1/4 of the progeny (4 out of 15 embryos) from mon^{tu244b} heterozygous carriers (Figs. 3C, D). *blf* expression was not affected in *vlad tepes* (vlt^{m651}) mutants (>40 embryos from heterozygous carriers analyzed) which are defective in the *gata1* transcription factor and form very few circulating blood cells (Lyons et al., 2002; Weinstein et al., 1996) (Fig. 3E). *blf* expression was not affected in *merlot/chablis* mutant embryos defective in the erythrocyte protein 4.1 (Shafizadeh et al., 2002; data not shown). These data suggest that Blf functions downstream of *clo* and TIF1γ but upstream of or independently from GATA1 and protein 4.1 in zebrafish hematopoiesis.

Morpholino knockdown of Blf

We used antisense morpholino oligonucleotides (MOs) to analyze the function of *blf* in embryogenesis (Nasevicius and Ekker, 2000). Injection of *blf* MOs resulted in undulations and curvature of axial structures, most notably the notochord (Fig. 4). *Blf*-MO-injected embryos (morphants) were much shorter than control uninjected embryos. *Blf* morphants also displayed delaminating cells from the dorsal ectoderm during mid-somitogenesis (Figs. 4E, H); most of these embryos died shortly after that. Three different *blf*-specific MOs caused the same phenotype, while a 5-base *blf*-mismatch MO and multiple *blf*-unrelated MOs never caused any of the described defects, demonstrating specificity of the *blf* knockdown phenotype (Fig. 4; data not shown).

Extension and convergence of axial tissues are perturbed in Blf morphants

To better understand the nature of the defects observed in *blf* morphants, we performed molecular analysis of different axial markers. The notochord in *blf* morphants was thicker and severely undulating as evident from the expression of *no tail (ntl)* and *sonic hedgehog (shh)* (Ekker et al., 1995; Schulte-Merker et al., 1994) (Figs. 5A–D). Analysis of *myod* expression (Weinberg et al., 1996) revealed that the somites were broader, more closely spaced and disorganized while the paraxial mesoderm was curved, following the shape of the notochord in *blf* morphants (Figs. 5E, F). The floorplate was expanded and undulating, similarly to the notochord, in *blf* morphants as analyzed by the expression of *shh*, *spondin1b (spon1b)* (Higashijima et al., 1997), and *foxA1* (Odenthal and Nusslein-Volhard, 1998) (Figs. 5C, D, G–J). In addition, the hypochord showed axial undulations as well (Figs. 5I, J). These results show that the axial tissues, including the axial and paraxial mesoderm, fail to extend and converge in *blf* morphants.

To assay convergent extension in *blf* morphants, we labeled cells by uncaging fluorescent dye at the shield stage. In control embryos (only injected with DMNB-caged fluorescein dextran), labeled lateral mesendodermal cells converged at the midline by the 2-somite stage (Figs. 6A, B). In *blf* morphants, lateral mesendodermal cells failed to converge at the midline and remained positioned laterally (Figs. 6C, D). These results confirm the defective convergence in *blf* morphants.

Neurulation and cell–cell adhesion defects in Blf morphants

To understand delamination of ectodermal cells observed in *blf* morphants, we analyzed the formation of neural tissue in greater detail. We used *hairy-related 4 (her4)* as a marker for neuroectoderm (Takke et al., 1999; Thisse et al., 2001) and *gata3* as a marker for non-neural ectoderm (Neave et al., 1995; Thisse et al., 2001). During early somitogenesis, the neuroectoderm was expanded in *blf* morphants, as evident from a wider expression area of *her4* in the neural plate (Figs. 7A, B, E, F) and a wider gap from which *gata3* expression was excluded (Figs. 7C, D, G, H). Also, during mid-somitogenesis, the expanded neural plate became split into two across the midline (Figs. 7I, J, M, N). The dorsal cells along the midline located inside of the split neural tube expressed the non-neural ectodermal marker *gata3* and the epidermal marker *cytokeratin E7* (Thisse et al., 2001) (Figs. 7G, H, K, L, O, P). The delaminating cells showed a very strong expression of *cytokeratin E7* demonstrating their epidermal nature (Figs. 7K, L, O, P). The expression of *crestin* in pre-migratory neural crest cells (Luo et al., 2001) was split into two stripes, following the shape of the split neural tube (Figs. 7Q, R). No or very little migration of the neural crest cells was observed in the *blf* morphants (Figs. 7S, T).

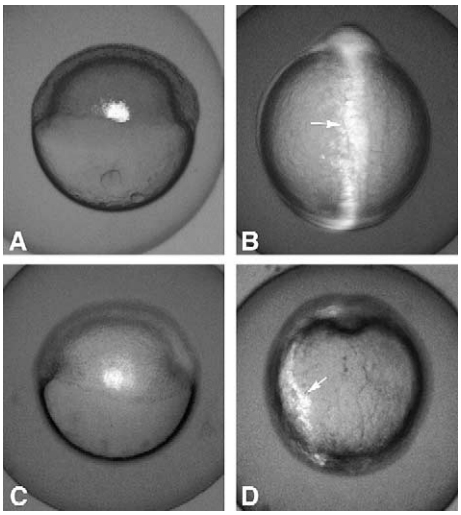

Fig. 6. Analysis of convergence in wt (A, B) and *blf* morphants (C, D) by uncaging DMNB-caged fluorescein-dextran in a group of cells within lateral mesendoderm. (A, C) A group of cells within lateral mesendoderm is labeled by the UV-photoactivation at the shield stage. Lateral view, dorsal is to the right. (B, D) The same embryo as in panels (A) or (C) at the 2-somite stage. Note that the labeled cells (arrows) have converged to the midline in the control (B) but not in the morphant embryo (D). Dorsal view, anterior is up.

The expanded neural plate observed in *blf* morphants during early somitogenesis may form due to either the failure of the neuroectodermal cells to converge or to increased neural induction. We distinguished between the two models by assaying a number of neural and ectodermal markers using real-time RT-PCR (Table 1). Expression of the neural markers *neurogenin (ngn1)* (Korzh et al., 1998) and *foxb1.2* (Odenthal and Nusslein-Volhard, 1998; Thisse et al., 2001) was not significantly affected in *blf* morphants (Table 1). Expression of the neural marker *her4* and neural crest-specific *crestin* was somewhat downregulated in *blf* morphants, while non-neural ectoderm-specific *gata3* and epidermal *cytokeratin E7* were slightly upregulated. The lack of increase in

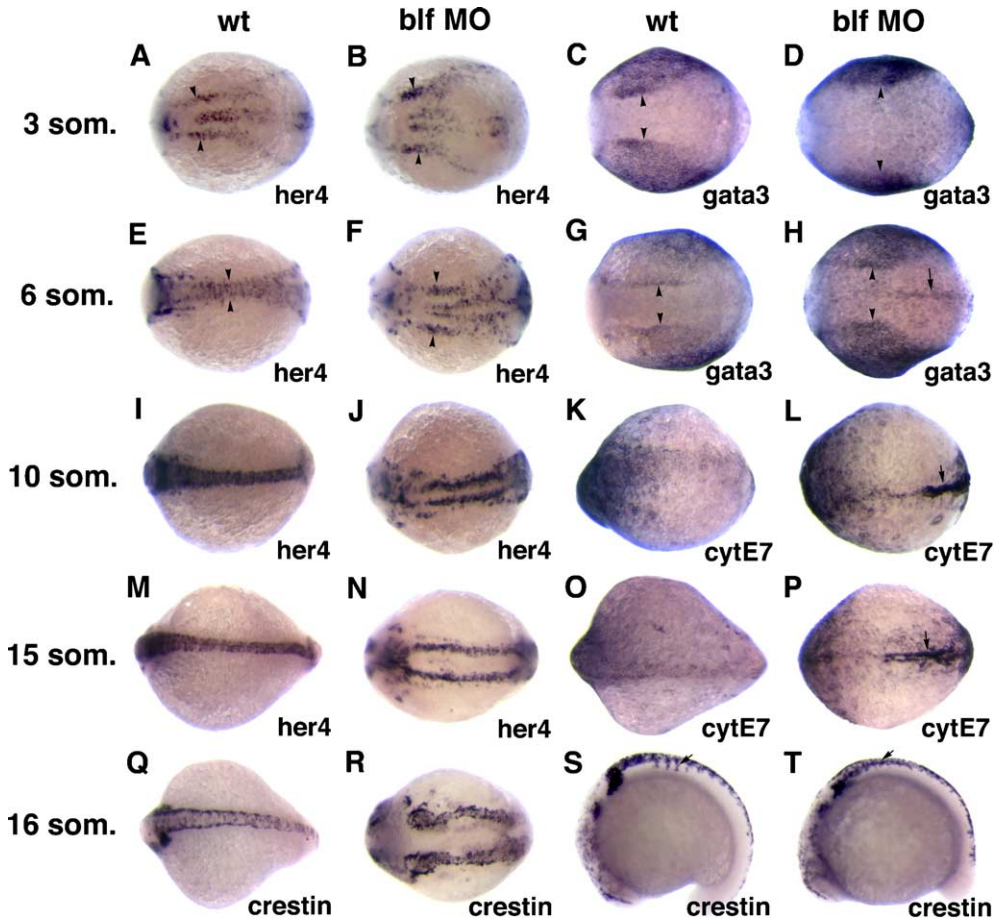

Fig. 7. In situ hybridization analysis of neural and ectodermal markers in *blf* morphants, injected with 2 ng of MO2. Dorsal view, anterior is to the left, except where noted. (A, B, E, F) *Hairy-related* transcription factor *her4* labels a subset of neural cells at the 3-somite (A, B) and 6-somite (E, F) stages. Note the expanded neural plate (arrowheads) in *blf* morphants (B, F), compared with uninjected control embryos (A, E). (C, D, G, H) GATA-family transcription factor *gata3* labels non-neural ectoderm at the 3-somite (C, D) and 6-somite (G, H) stages. Note that the gap in *gata3* expression which corresponds to the neural plate (arrowheads), is wider in *blf* morphants (D, H), compared with uninjected control embryos (C, G). Additional *gata3*-expressing cells are observed at the midline of *blf* morphants (arrow, H). (I, J, M, N) *Her4* expression labels neural tube at the 10-somite (I, J) and 15-somite (M, N) stages. Note the bilaterally split neural tube in *blf* morphants (J, N), compared with uninjected control embryos (I, M). (K, L, O, P) *Cytokeratin E7* expression labels epidermal cells at the 10-somite (K, L) and 15-somite (O, P) stages. Note the strong enrichment in cytokeratin expression in the delaminating cells of dorsal posterior ectoderm in *blf* morphants (arrows in L, P), compared with uninjected control embryos (K, O). (Q, R) *Crestin* expression labels neural crest cells at the 16-somite stage. Note two bilateral stripes of neural crest cells in *blf* morphants (R) compared with the single stripe in control uninjected embryos (Q). (S, T) *Crestin* expression, 16-somite stage. Note the absence of the intersomitic bands of migrating neural crest cells (arrow) in *blf* morphants (T), compared with uninjected control embryos (S).

neural marker expression in *blf* morphants supports the hypothesis that the observed neurulation defects in *blf* morphants are caused by defective morphogenetic movements and not by inductive events. Downregulation of certain neural markers and upregulation of genes specific to non-neural ectoderm is consistent with a subset of neural cells adopting epidermal fate and delaminating in *blf* morphants (see Discussion).

We investigated formation of dorsal mesoderm during gastrulation by analyzing *goosecoid (gsc)* expression

Table 1
Normalized expression ratio of neural and ectodermal markers in *blf* morphants vs. wild-type embryos as analyzed by real-time RT-PCR

Gene	Normalized expression ratio in *blf* morphants	Expression pattern and stage of analysis
neurogenin 1 (ngn1)	0.92 ± 0.22	Subset of brain and spinal chord (Korzh et al., 1998); 10 somites
forkhead box B1.2 (foxb1.2)	1.11 ± 0.23	Brain, ventral spinal chord and paraxial mesoderm (Thisse et al., 2001); 10 somites
hairy related 4 (her4)	0.55 ± 0.12	Brain, spinal chord (Thisse et al., 2001); 10 somites
crestin	0.60 ± 0.07	Neural crest (Luo et al., 2001); 10 somites
gata3	1.95 ± 0.17	Non-neural ectoderm (Thisse et al., 2001); 4 somites
cytokeratin E7	1.59 ± 0.38	Epidermis (Thisse et al., 2001); 4 somites

(Stachel et al., 1993). No significant difference in *gsc* expression was found between wild-type embryos and *blf* morphants at the 60% epiboly stage (data not shown).

Given the expression of *blf* in hematopoietic cells at later stages, we performed extensive analysis of blood cell formation in the *blf* morphants. We used moderate doses of MO2 and MO3 morpholinos which allowed survival of the injected embryos until 36 hpf or longer. Both MO2- and MO3-injected embryos formed approximately normal numbers of blood cells in circulation as determined by visual observation and *o*-dianisidine heme staining (Detrich et al., 1995) (data not shown). At 20–24 hpf, expression of the early hematopoietic markers *gata1*, *gata2*, *tal1/scl*, *cmyb*, and *ikaros* was not significantly affected as analyzed by in situ hybridization and real-time RT-PCR (data not shown). These data illustrate that the knockdown of *blf* did not have a significant effect on the formation of primitive red blood or lymphoid cells and that *blf* may play a redundant role in this process (see Discussion). We also addressed the possibility that *blf* and *draculin* may play redundant roles in hematopoiesis because of their high sequence homology and overlapping expression in the ICM region (Herbomel et al., 1999). However, injection of *blf* and *draculin* MO mixture did not result in any significant hematopoietic defects as determined by the morphological analysis (data not shown).

Discussion

In this study, we isolated a zebrafish cDNA encoding a novel 15-zinc finger domain protein, Bloody Fingers. *blf* was expressed strongly and ubiquitously soon after the start of zygotic transcription. During gastrulation, *blf* became gradually restricted to the posterior dorsolateral mesoderm area. During somitogenesis, *blf* expression in the dorsolateral mesoderm disappeared, and later reappeared in hematopoietic progenitor cells. We studied the function of *blf* in embryonic development using morpholinos. MO knockdown of *blf* interfered with the extension and convergence of axial tissues. *Blf* morphants displayed split neural tube, characteristic of spina bifida birth defects in humans. In addition, *blf* morphants displayed delaminating dorsal ectodermal cells. These results argue for the involvement of *blf* in convergent extension and provide the first zebrafish model for spina bifida.

The isolated *blf* cDNA encodes a zinc finger protein displaying an unusual structure of 15 sequential zinc fingers spanning almost the entire length of the protein. We did not find any other vertebrate protein with a similar structure of fifteen zinc fingers. However, proteins with multiple zinc finger domains have been previously known, such as the Roaz protein which contains 29 sequential zinc fingers (Tsai and Reed, 1997). It is possible that the Blf protein is unique to zebrafish. A more likely hypothesis is that the Blf protein diverged during evolution far enough to have a different structure from its orthologue in other vertebrates. A structurally similar zinc finger protein, Draculin, has been found in zebrafish. Although Dra contains 13 zinc finger domains while Blf has 15, the spacing between Cys and His residues within each finger, and the linker domains between the fingers are highly conserved between the two proteins. Expression domains of *dra* and *blf* also partially overlap among hematopoietic progenitors in the ventral mesoderm (Herbomel et al., 1999). The zebrafish genome has undergone partial duplication in recent evolutionary history (Postlethwait et al., 1999). It is possible that *dra* and *blf* had a common gene precursor and diverged after the duplication event.

MO knockdown of Blf resulted in undulating axial tissues. Undulations may happen if convergence of axial and paraxial tissues happens at different rates. As axial tissues try to extend, they are restricted by the somites, and buckle under tension. These defects are similar to phenotypes observed due to the loss of function of *wnt5*, *fz2*, *knypek*, *strabismus*, and *prickle* genes, involved in the *wnt* non-canonical signaling pathway. Further research will have to establish the possible link between *blf* and the PCP pathway. In addition to the defects in convergent extension, *blf* morphants showed severe neurulation defects such as a split neural tube and delamination of cells in the dorsal ectoderm. CE and neurulation are tightly linked. Involvement of PCP pathway genes in both CE and neurulation has been described in other vertebrate organisms (Ueno and Greene, 2003). However, none of the zebrafish PCP mutants or morphants have been reported to display neurulation defects. It is possible that the gastrulation defects mask later neurulation defects or that PCP family members are redundant in zebrafish.

We propose a model which describes how defective convergent extension in *blf* morphants could lead to the observed neurulation defects and cell delamination. Because of the defective CE in *blf* morphants, their neural plate is thinner and wider than in wild-type embryos (Fig. 8). Epidermal cells are normally located on both sides of the neural tissue at the beginning of neurulation. As neural keel formation takes place, the epidermis converges to completely envelope the neural plate (Strahle and Blader, 1994). However, in *blf* morphants, the neural plate is wider and convergence is defective; therefore, the epidermis fails to envelope the entire neural plate. The outermost neural cells, which are not enveloped by epidermis, adopt epidermal cell fate 'by default' due to the lack of contact with neighboring cells (Fig. 8). Alternatively, induction of the dorsal neural tissue may be compromised, resulting in a subset of these cells adopting epidermal fate. Delamination could happen because the 'neural epidermal' cells are not expressing proper cell–cell adhesion proteins. This model is consistent with all our observations, including: *blf* morphants display a wider and thinner neural plate; the delaminating cells are located exactly in-between the stripes of the divided neural

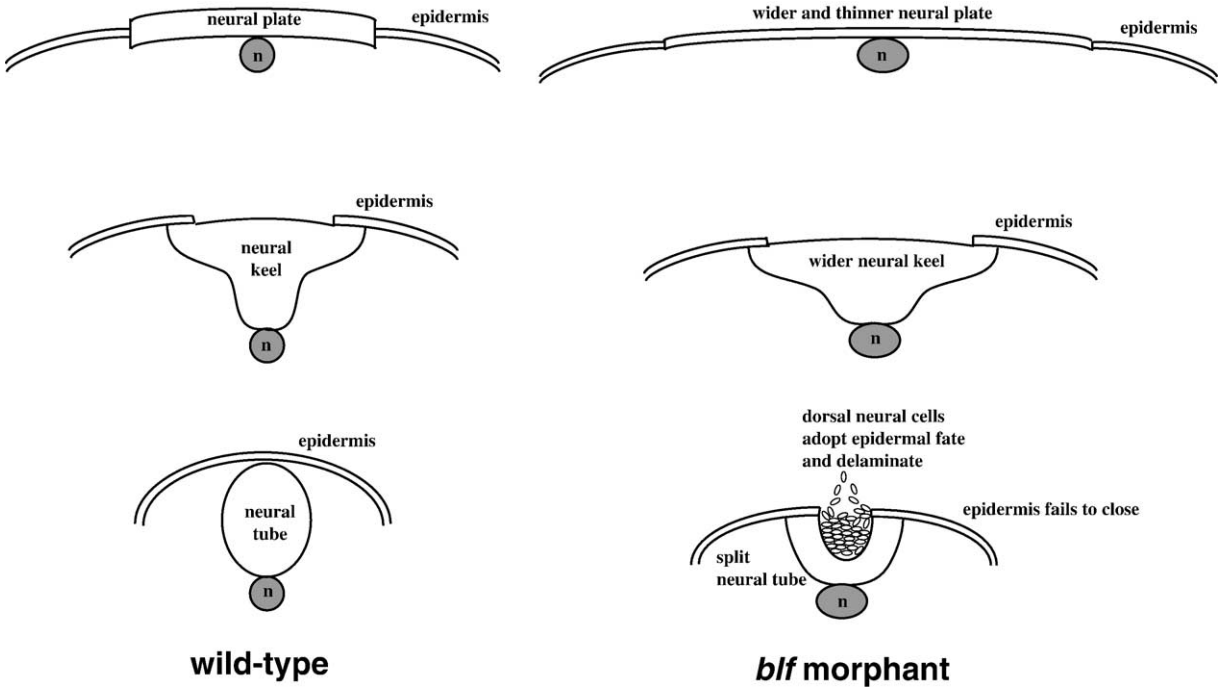

Fig. 8. Neurulation model in wild-type embryos and *blf* morphants.

tube; and these delaminating cells display strong expression of the epidermal marker *cytokeratin E7*. Downregulation of the neural markers *her4* and *crestin* as well as upregulation of the ectodermal markers *foxb1.2* and *cytE7* in *blf* morphants as observed by real-time RT-PCR also support this model. Neural markers *ngn1* and *foxb1.2* are not much affected, possibly because *ngn1* is expressed only in a subset of neural cells (Korzh et al., 1998), while *foxb1.2* is excluded from the dorsal and posterior neural plate (Thisse et al., 2001), where delamination is the most pronounced.

Starting from mid-somitogenesis until approximately 28 hpf, *blf* is localized exclusively to the region of primitive hematopoiesis. Despite this expression pattern, we failed to detect any hematopoietic defects in *blf* morphants. Because *blf* morphants with severe CE and neurulation defects die during somitogenesis, we were limited to using lower MO doses to investigate hematopoiesis. It is possible that lower MO doses did not cause sufficient inhibition to observe a hematopoiesis-related phenotype. Alternatively, the plausible role of *blf* in blood formation could be redundant. We attempted to address the possible redundancy between *blf* and *dra* by injecting a mixture of MOs directed against both genes but did not detect any blood-related phenotype. There are multiple other zinc finger proteins expressed in the region of primitive hematopoiesis, e.g., three different members of the Kruppel-like factor family (Oates et al., 2001). Therefore, there are many possibilities for the functional redundancy between Blf and other proteins.

In summary, we describe a function of a novel zinc finger protein, Bloody Fingers, in regulating morphogenetic movements during gastrulation and neurulation. In addition to expanding our knowledge of the mechanisms regulating these fundamental developmental processes, this study establishes zebrafish as a model for spina bifida, a common neural tube birth defect in humans.

Acknowledgments

This research was supported by the NIH RO1 grant #DK54508 to S. Lin. We also thank the Zebrafish International Resource Center for the cDNA probes which was supported by grant #RR12546 from the NIH-NCRR.

References

Carreira-Barbosa, F., Concha, M.L., Takeuchi, M., Ueno, N., Wilson, S.W., Tada, M., 2003. Prickle 1 regulates cell movements during gastrulation and neuronal migration in zebrafish. Development 130, 4037–4046.

Copp, A.J., Greene, N.D., Murdoch, J.N., 2003. The genetic basis of mammalian neurulation. Nat. Rev., Genet. 4, 784–793.

Darken, R.S., Scola, A.M., Rakeman, A.S., Das, G., Mlodzik, M., Wilson, P.A., 2002. The planar polarity gene strabismus regulates convergent extension movements in *Xenopus*. EMBO J. 21, 976–985.

Detrich III, H.W., Kieran, M.W., Chan, F.Y., Barone, L.M., Yee, K., Rundstadler, J.A., Pratt, S., Ransom, D., Zon, L.I., 1995. Intra-embryonic hematopoietic cell migration during vertebrate development. Proc. Natl. Acad. Sci. U. S. A. 92, 10713–10717.

Ekker, S.C., Ungar, A.R., Greenstein, P., von Kessler, D.P., Porter, J.A., Moon, R.T., Beachy, P.A., 1995. Patterning activities of vertebrate hedgehog proteins in the developing eye and brain. Curr. Biol. 5, 944–955.

Finerty Jr., P.J., Bass, B.L., 1997. A *Xenopus* zinc finger protein that specifically binds dsRNA and RNA–DNA hybrids. J. Mol. Biol. 271, 195–208.

Friesen, W.J., Darby, M.K., 1998. Specific RNA binding proteins constructed from zinc fingers. Nat. Struct. Biol. 5, 543–546.

Goto, T., Keller, R., 2002. The planar cell polarity gene strabismus regulates convergence and extension and neural fold closure in *Xenopus*. Dev. Biol. 247, 165–181.

Hammerschmidt, M., Pelegri, F., Mullins, M.C., Kane, D.A., Brand, M., van Eeden, F.J., Furutani-Seiki, M., Granato, M., Haffter, P., Heisenberg, C.P., Jiang, Y.J., Kelsh, R.N., Odenthal, J., Warga, R.M., Nusslein-Volhard, C., 1996. Mutations affecting morphogenesis during gastrulation and tail formation in the zebrafish, *Danio rerio*. Development 123, 143–151.

Heisenberg, C.P., Tada, M., 2002. Zebrafish gastrulation movements: bridging cell and developmental biology. Semin. Cell Dev. Biol. 13, 471–479.

Heisenberg, C.P., Tada, M., Rauch, G.J., Saude, L., Concha, M.L., Geisler, R., Stemple, D.L., Smith, J.C., Wilson, S.W., 2000. Silberblick/Wnt11 mediates convergent extension movements during zebrafish gastrulation. Nature 405, 76–81.

Herbomel, P., Thisse, B., Thisse, C., 1999. Ontogeny and behaviour of early macrophages in the zebrafish embryo. Development 126, 3735–3745.

Higashijima, S., Nose, A., Eguchi, G., Hotta, Y., Okamoto, H., 1997. Mindin/F-spondin family: novel ECM proteins expressed in the zebrafish embryonic axis. Dev. Biol. 192, 211–227.

Hoppler, S., Brown, J.D., Moon, R.T., 1996. Expression of a dominant-negative Wnt blocks induction of MyoD in *Xenopus* embryos. Genes Dev. 10, 2805–2817.

Hopwood, N.D., Pluck, A., Gurdon, J.B., 1989. MyoD expression in the forming somites is an early response to mesoderm induction in *Xenopus* embryos. EMBO J. 8, 3409–3417.

Hyatt, T.M., Ekker, S.C., 1999. Vectors and techniques for ectopic gene expression in zebrafish. Methods Cell Biol. 59, 117–126.

Iuchi, S., 2001. Three classes of C2H2 zinc finger proteins. Cell. Mol. Life Sci. 58, 625–635.

Jessen, J.R., Topczewski, J., Bingham, S., Sepich, D.S., Marlow, F., Chandrasekhar, A., Solnica-Krezel, L., 2002. Zebrafish trilobite identifies new roles for Strabismus in gastrulation and neuronal movements. Nat. Cell Biol. 4, 610–615.

Jowett, T., 1999. Analysis of protein and gene expression. Methods Cell Biol. 59, 63–85.

Kelley, C.M., Ikeda, T., Koipally, J., Avitahl, N., Wu, L., Georgopoulos, K., Morgan, B.A., 1998. Helios, a novel dimerization partner of Ikaros expressed in the earliest hematopoietic progenitors. Curr. Biol. 8, 508–515.

Kilian, B., Mansukoski, H., Barbosa, F.C., Ulrich, F., Tada, M., Heisenberg, C.P., 2003. The role of Ppt/Wnt5 in regulating cell shape and movement during zebrafish gastrulation. Mech. Dev. 120, 467–476.

Kimmel, C.B., Ballard, W.W., Kimmel, S.R., Ullmann, B., Schilling, T.F., 1995. Stages of embryonic development of the zebrafish. Dev. Dyn. 203, 253–310.

Korzh, V., Sleptsova, I., Liao, J., He, J., Gong, Z., 1998. Expression of zebrafish bHLH genes ngn1 and nrd defines distinct stages of neural differentiation. Dev. Dyn. 213, 92–104.

Liao, E.C., Paw, B.H., Oates, A.C., Pratt, S.J., Postlethwait, J.H., Zon, L.I., 1998. SCL/Tal-1 transcription factor acts downstream of cloche to specify hematopoietic and vascular progenitors in zebrafish. Genes Dev. 12, 621–626.

Long, Q., Huang, H., Shafizadeh, E., Liu, N., Lin, S., 2000. Stimulation of erythropoiesis by inhibiting a new hematopoietic death receptor in transgenic zebrafish. Nat. Cell Biol. 2, 549–552.

Lowery, L.A., Sive, H., 2004. Strategies of vertebrate neurulation and a re-evaluation of teleost neural-tube formation. Mech. Dev. 121, 1189–1197.

Luo, R., An, M., Arduini, B.L., Henion, P.D., 2001. Specific pan-neural crest expression of zebrafish Crestin throughout embryonic development. Dev. Dyn. 220, 169–174.

Lyons, S.E., Lawson, N.D., Lei, L., Bennett, P.E., Weinstein, B.M., Liu, P.P., 2002. A nonsense mutation in zebrafish gata1 causes the bloodless phenotype in vlad tepes. Proc. Natl. Acad. Sci. U. S. A. 99, 5454–5459.

Marlow, F., Zwartkruis, F., Malicki, J., Neuhauss, S.C., Abbas, L., Weaver, M., Driever, W., Solnica-Krezel, L., 1998. Functional interactions of genes mediating convergent extension, knypek and trilobite, during the partitioning of the eye primordium in zebrafish. Dev. Biol. 203, 382–399.

Morgan, B., Sun, L., Avitahl, N., Andrikopoulos, K., Ikeda, T., Gonzales, E., Wu, P., Neben, S., Georgopoulos, K., 1997. Aiolos, a lymphoid restricted transcription factor that interacts with Ikaros to regulate lymphocyte differentiation. EMBO J. 16, 2004–2013.

Nasevicius, A., Ekker, S.C., 2000. Effective targeted gene 'knockdown' in zebrafish. Nat. Genet. 26, 216–220.

Neave, B., Rodaway, A., Wilson, S.W., Patient, R., Holder, N., 1995. Expression of zebrafish GATA 3 (gta3) during gastrulation and neurulation suggests a role in the specification of cell fate. Mech. Dev. 51, 169–182.

Oates, A.C., Pratt, S.J., Vail, B., Yan, Y., Ho, R.K., Johnson, S.L., Postlethwait, J.H., Zon, L.I., 2001. The zebrafish klf gene family. Blood 98, 1792–1801.

Odenthal, J., Nusslein-Volhard, C., 1998. fork head domain genes in zebrafish. Dev. Genes Evol. 208, 245–258.

Papan, C., Campos-Ortega, J.A., 1994. On the formation of the neural keel and neural tube in the zebrafish *Danio (Brachydanio) rerio*. Roux's Arch. Dev. Biol. 203, 178–186.

Park, M., Moon, R.T., 2002. The planar cell-polarity gene stbm regulates cell behaviour and cell fate in vertebrate embryos. Nat. Cell Biol. 4, 20–25.

Postlethwait, J., Amores, A., Force, A., Yan, Y.L., 1999. The zebrafish genome. Methods Cell Biol. 60, 149–163.

Ransom, D.G., Bahary, N., Niss, K., Traver, D., Burns, C., Trede, N.S., Paffett-Lugassy, N., Saganic, W.J., Lim, C.A., Hersey, C., Zhou, Y., Barut, B.A., Lin, S., Kingsley, P.D., Palis, J., Orkin, S.H., Zon, L.I., 2004. The zebrafish moonshine gene encodes transcriptional intermediary factor 1gamma, an essential regulator of hematopoiesis. PLoS Biol. 2 (8), E237.

Ransom, D.G., Haffter, P., Odenthal, J., Brownlie, A., Vogelsang, E., Kelsh, R.N., Brand, M., van Eeden, F.J., Furutani-Seiki, M., Granato, M., Hammerschmidt, M., Heisenberg, C.P., Jiang, Y.J., Kane, D.A., Mullins, M.C., Nusslein-Volhard, C., 1996. Characterization of zebrafish mutants with defects in embryonic hematopoiesis. Development 123, 311–319.

Rauch, G.J., Hammerschmidt, M., Blader, P., Schauerte, H.E., Strahle, U., Ingham, P.W., McMahon, A.P., Haffter, P., 1997. Wnt5 is required for tail formation in the zebrafish embryo. Cold Spring Harbor Symp. Quant. Biol. 62, 227–234.

Reichenbach, A., Schaaf, P., Schneider, H., 1990. Primary neurulation in teleosts. Evidence for epithelial genesis of central nervous tissue as in other vertebrates. J. Hirnforsch. 31, 152–158.

Schulte-Merker, S., van Eeden, F.J., Halpern, M.E., Kimmel, C.B., Nusslein-Volhard, C., 1994. no tail (ntl) is the zebrafish homologue of the mouse T (Brachyury) gene. Development 120, 1009–1015.

Shafizadeh, E., Paw, B.H., Foott, H., Liao, E.C., Barut, B.A., Cope, J.J., Zon, L.I., Lin, S., 2002. Characterization of zebrafish merlot/chablis as non-mammalian vertebrate models for severe congenital anemia due to protein 4.1 deficiency. Development 129, 4359–4370.

Shulman, J.M., Perrimon, N., Axelrod, J.D., 1998. Frizzled signaling and the developmental control of cell polarity. Trends Genet. 14, 452–458.

Solnica-Krezel, L., Stemple, D.L., Mountcastle-Shah, E., Rangini, Z., Neuhauss, S.C., Malicki, J., Schier, A.F., Stainier, D.Y., Zwartkruis, F., Abdelilah, S., Driever, W., 1996. Mutations affecting cell fates and cellular rearrangements during gastrulation in zebrafish. Development 123, 67–80.

Stachel, S.E., Grunwald, D.J., Myers, P.Z., 1993. Lithium perturbation and goosecoid expression identify a dorsal specification pathway in the pregastrula zebrafish. Development 117, 1261–1274.

Stainier, D.Y., Weinstein, B.M., Detrich III, H.W., Zon, L.I., Fishman, M.C.,

1995. Cloche, an early acting zebrafish gene, is required by both the endothelial and hematopoietic lineages. Development 121, 3141–3150.

Stainier, D.Y., Fouquet, B., Chen, J.N., Warren, K.S., Weinstein, B.M., Meiler, S.E., Mohideen, M.A., Neuhauss, S.C., Solnica-Krezel, L., Schier, A.F., Zwartkruis, F., Stemple, D.L., Malicki, J., Driever, W., Fishman, M.C., 1996. Mutations affecting the formation and function of the cardiovascular system in the zebrafish embryo. Development 123, 285–292.

Strahle, U., Blader, P., 1994. Early neurogenesis in the zebrafish embryo. FASEB J. 8, 692–698.

Sumanas, S., Strege, P., Heasman, J., Ekker, S.C., 2000. The putative wnt receptor *Xenopus* frizzled-7 functions upstream of beta-catenin in vertebrate dorsoventral mesoderm patterning. Development 127, 1981–1990.

Sumanas, S., Kim, H.J., Hermanson, S., Ekker, S.C., 2001. Zebrafish frizzled-2 morphant displays defects in body axis elongation. Genesis 30, 114–118.

Takeuchi, M., Nakabayashi, J., Sakaguchi, T., Yamamoto, T.S., Takahashi, H., Takeda, H., Ueno, N., 2003. The prickle-related gene in vertebrates is essential for gastrulation cell movements. Curr. Biol. 13, 674–679.

Takke, C., Dornseifer, P., von Weizsacker, E., Campos-Ortega, J.A., 1999. her4, a zebrafish homologue of the *Drosophila* neurogenic gene E(spl), is a target of notch signalling. Development 126, 1811–1821.

Thisse, B., Pfumio, S., Fürthauer, M., Loppin B., Heyer, V., Degrave, A., Woehl, R., Lux, A., Steffan, T., Charbonnier, X.Q., Thisse, C., 2001. Expression of the zebrafish genome during embryogenesis. ZFIN online publication.

Thompson, M.A., Ransom, D.G., Pratt, S.J., MacLennan, H., Kieran, M.W., Detrich III, H.W., Vail, B., Huber, T.L., Paw, B., Brownlie, A.J., Oates, A.C., Fritz, A., Gates, M.A., Amores, A., Bahary, N., Talbot, W.S., Her, H., Beier, D.R., Postlethwait, J.H., Zon, L.I., 1998. The cloche and spadetail genes differentially affect hematopoiesis and vasculogenesis. Dev. Biol. 197, 248–269.

Topczewski, J., Sepich, D.S., Myers, D.C., Walker, C., Amores, A., Lele, Z., Hammerschmidt, M., Postlethwait, J., Solnica-Krezel, L., 2001. The zebrafish glypican knypek controls cell polarity during gastrulation movements of convergent extension. Dev. Cell 1, 251–264.

Tsai, R.Y., Reed, R.R., 1997. Cloning and functional characterization of Roaz, a zinc finger protein that interacts with O/E-1 to regulate gene expression: implications for olfactory neuronal development. J. Neurosci. 17, 4159–4169.

Ueno, N., Greene, N.D., 2003. Planar cell polarity genes and neural tube closure. Birth Defects Res., Part C Embryo Today 69, 318–324.

Veeman, M.T., Slusarski, D.C., Kaykas, A., Louie, S.H., Moon, R.T., 2003. Zebrafish prickle, a modulator of noncanonical Wnt/Fz signaling, regulates gastrulation movements. Curr. Biol. 13, 680–685.

Wallingford, J.B., Harland, R.M., 2002. Neural tube closure requires Dishevelled-dependent convergent extension of the midline. Development 129, 5815–5825.

Wallingford, J.B., Rowning, B.A., Vogeli, K.M., Rothbacher, U., Fraser, S.E., Harland, R.M., 2000. Dishevelled controls cell polarity during *Xenopus* gastrulation. Nature 405, 81–85.

Weinberg, E.S., Allende, M.L., Kelly, C.S., Abdelhamid, A., Murakami, T., Andermann, P., Doerre, O.G., Grunwald, D.J., Riggleman, B., 1996. Developmental regulation of zebrafish MyoD in wild-type, no tail and spadetail embryos. Development 122, 271–280.

Weinstein, B.M., Schier, A.F., Abdelilah, S., Malicki, J., Solnica-Krezel, L., Stemple, D.L., Stainier, D.Y., Zwartkruis, F., Driever, W., Fishman, M.C., 1996. Hematopoietic mutations in the zebrafish. Development 123, 303–309.

Willett, C.E., Kawasaki, H., Amemiya, C.T., Lin, S., Steiner, L.A., 2001. Ikaros expression as a marker for lymphoid progenitors during zebrafish development. Dev. Dyn. 222, 694–698.

Winklbauer, R., Medina, A., Swain, R.K., Steinbeisser, H., 2001. Frizzled-7 signalling controls tissue separation during *Xenopus* gastrulation. Nature 413, 856–860.

Yamashita, S., Miyagi, C., Carmany-Rampey, A., Shimizu, T., Fujii, R., Schier, A.F., Hirano, T., 2002. Stat3 controls cell movements during zebrafish gastrulation. Dev. Cell 2, 363–375.